1-1-2018

Comparing Positively and Negatively Charged Distonic Radical Ions in Phenylperoxyl Forming Reactions

Peggy Williams
Queensland University of Technology

David L. Marshall
Queensland University of Technology, dlm418@uowmail.edu.au

Berwyck L. J Poad
Queensland University of Technology, bpoad@uow.edu.au

Venkateswara Narreddula
Queensland University of Technology

Benjamin B. Kirk
University of Wollongong, bkirk@uow.edu.au

See next page for additional authors

Publication Details Citation

Comparing Positively and Negatively Charged Distonic Radical Ions in Phenylperoxyl Forming Reactions

Abstract

In the gas phase, arylperoxyl forming reactions play a significant role in low-temperature combustion and atmospheric processing of volatile organic compounds. We have previously demonstrated the application of charge-tagged phenyl radicals to explore the outcomes of these reactions using ion trap mass spectrometry. Here, we present a side-by-side comparison of rates and product distributions from the reaction of positively and negatively charge tagged phenyl radicals with dioxygen. The negatively charged distonic radical ions are found to react with significantly greater efficiency than their positively charged analogues. The product distributions of the anion reactions favor products of phenylperoxyl radical decomposition (e.g., phenoxyl radicals and cyclopentadienone), while the comparable fixed-charge cations yield the stabilized phenylperoxyl radical. Electronic structure calculations rationalize these differences as arising from the influence of the charged moiety on the energetics of rate-determining transition states and reaction intermediates within the phenylperoxyl reaction manifold and predict that this influence could extend to intra-molecular charge-radical separations of up to 14.5 Å. Experimental observations of reactions of the novel 4-(1-carboxylatoadamantyl)phenyl radical anion confirm that the influence of the charge on both rate and product distribution can be modulated by increasing the rigidly imposed separation between charge and radical sites. These findings provide a generalizable framework for predicting the influence of charged groups on polarizable radicals in gas phase distonic radical ions.

Publication Details

Authors

Peggy Williams, David L. Marshall, Berwyck L. J Poad, Venkateswara Narreddula, Benjamin B. Kirk, Adam J. Trevitt, and Stephen J. Blanksby

Comparing positively- and negatively-charged distonic radical ions in phenylperoxyl forming reactions[¶]

Peggy E. Williams[1][†], David L. Marshall[1], Berwyck L. J. Poad[1], Venkateswara R. Narreddula[1], Benjamin B. Kirk[2], Adam J. Trevitt[2], Stephen J. Blanksby[1][*]

[1] Central Analytical Research Facility, Institute for Future Environments, Queensland University of Technology, QLD Australia

[2] School of Chemistry, University of Wollongong, NSW Australia

[*]Email: stephen.blanksby@qut.edu.au

[†] Current address: Failure and Materials Analysis Branch, Flight Systems Division, Naval Surface Warfare Center Crane, Indiana, USA

[¶] This manuscript is in honor of Prof. Ryan R. Julian winner of the 2017 ASMS Biemann Medal. Prof. Julian's contributions to the field of radical ion chemistry and his friendship have inspired our research endeavours.

Abstract

In the gas phase, arylperoxyl forming reactions play a significant role in low temperature combustion and atmospheric processing of volatile organic compounds. We have previously demonstrated the application of charge-tagged phenyl radicals to explore the outcomes of these reactions using ion trap mass spectrometry. Here we present a side-by-side comparison of rates and product distributions from the reaction of positively- and negatively-charge tagged phenyl radicals with dioxygen. The negatively charged distonic radical ions are found to react with significantly greater efficiency than their positively charged analogues. The product distribution of the anion reactions favor products of phenylperoxyl radical decomposition (*e.g.*, phenoxyl radicals and cyclopentadienone) while the comparable fixed-charge cations yield the stabilized phenylperoxyl radical. Electronic structure calculations rationalize these differences as arising from the influence of the charged moiety on the energetics of rate-determining transition states and reaction intermediates within the phenylperoxyl reaction manifold and predict that this influence could extend to intra-molecular charge-radical separations of up to 14.5 Å. Experimental observations of reactions of the novel 4-(1-carboxylatoadamantyl)phenyl radical anion confirm that the influence of the charge on both rate and product distribution can be modulated by increasing the rigidly imposed separation between charge and radical sites. These findings provide a generalizable framework for predicting the influence of charged groups on polarizable radicals in gas phase distonic radical ions.

Keywords

Introduction

Organic peroxyl radicals (ROO•) are an important class of reaction intermediate in the mechanisms of low-temperature combustion as well as in the oxidative processing of volatile organic compounds in the Earth's lower atmosphere [1, 2]. Despite the importance of organic peroxyl radicals in these chemistries the direct observation of peroxyl formation and decomposition reactions has remained a significant challenge for conventional experimental techniques. This is because, in the gas phase, peroxyl radicals are typically generated in very low concentrations and have a high propensity for subsequent reaction – including decomposition and self-reactions – resulting in relatively short lifetimes. Building on the pioneering work by Kenttämaa and co-workers [3-6], a number of groups – including our own – have exploited the distonic radical ion approach for studying the chemistry of organic peroxyl radicals in the gas phase using ion cyclotron resonance and ion-trap mass spectrometries [7-16].

Distonic ions have radical centers that are spatially separated from the charge site [17, 18]. This class of radicals ions have been much-less studied than conventional radical ions (where charge and radical are co-localized) since the latter are more commonly produced by traditional ionization techniques; namely, electron and photo-ionization [19]. Despite requiring greater regiochemical control in their synthesis, distonic ions can represent the global minimum on the radical ion surface and, moreover, provide an attractive model for studying radical reactivity by mass spectrometry. The benefits in deploying this strategy lie in the ability to generate high concentrations of reactive species without complicating self- or cross-reactions (owing to Coulombic repulsion of like-charges), combined with the power to cleanly isolate and identify reaction products through changes in mass-to-charge ratio (*m/z*) [6, 20]. The role of the charge itself in modulating the reactivity of the remote radicals however, has been the subject of recent interest with computational studies indicating that polarizable peroxyl and nitroxyl radicals may be stabilized significantly by the presence of a negative charge in a distonic radical anion [21, 22]. Stabilization of the radical anion by up to

5 kcal mol^{-1} relative to neutral radical analogues has been reported; with smaller, but still significant effects, computed over intra-molecular distances >10 Å. These findings suggest that radical reactivity may be modulated by the presence of a remote charged moiety with both the charge polarity and charge-radical separation being key determinants of reaction outcomes.

We have previously reported the application of the distonic ion approach to the examination of the reactivity of phenyl radicals with dioxygen [15]. These investigations uncovered a unique route to the generation and isolation of elusive phenylperoxyl radicals that were then subjected to interrogation by photodissociation action spectroscopy [23]. A key observation by Kirk *et al.* was that reaction efficiencies and product distributions of the aryl radicals were affected by the polarity of the charged moiety [15]. For example, reaction of the *p*-(*N,N,N*-trimethylammonium)phenyl radical cation with dioxygen afforded the corresponding [M+O$_2$]$^{•+}$ phenylperoxyl radical cation as the major product with an overall efficiency of 4.9% (of the collision rate). In contrast, the *p*-carboxylatophenyl radical anion was observed to react with an efficiency of 9.2% producing an array of products, including [M+O$_2$-O]$^{•-}$ and [M+O$_2$-CHO]$^{•-}$, arising from decomposition of a phenylperoxyl radical intermediate [15]. To rationalise these observations, we describe here a systematic experimental and theoretical investigation of the effect of (i) charge-tag polarity and (ii) charge-radical separation on the phenylperoxyl-forming reactions of distonic radical ions. Seven charge-tagged phenyl radicals (**1 – 7,** Chart 1) were selected for this study in order to provide: good overlap with previously described distonic ion systems (**1**, **2**, **5** and **6**) [6, 15]; non-delocalizable negative charge carriers through the use of hypervalent trifluoroborate anion moieties (**3** and **4**) and; increased separation between charge and phenyl radical sites in the scaffold of the 4-(1-carboxylatoadamantyl)phenyl radical anion (**7**). The reaction efficiencies and product distributions of these radical ions are presented along with electronic structure calculations that extend the exploration of charge-radical effects beyond the experimental test set.
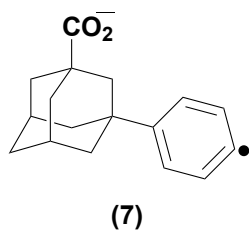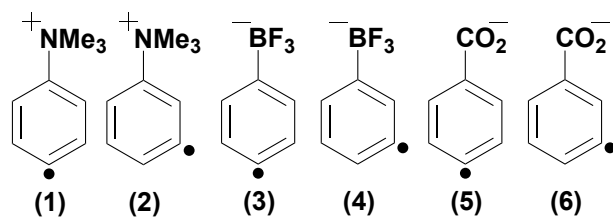
Chart 1. Structures of the 7 distonic radical ions explored in this study.

Methods

Materials

3-iodo-*N,N,N*-trimethylanilinium iodide and 4-iodo-*N,N,N*-trimethylanilinium iodide were previously synthesized according to literature methods [15, 24, 25]. 3-(4-iodophenyl) adamantane-1-carboxylic acid was obtained from VBR Molecules (Hyderabad, India). Potassium 3-iodophenyltrifluoroborate (≥97%) and potassium 4-iodophenyltrifluoroborate (≥97%) were purchased from Advanced Molecular Technologies (Scoresby, Australia). 3-iodobenzoic acid (98%), 4-iodobenzoic acid (98%) and dimethyl disulfide (98%) were purchased from Sigma-Aldrich (St. Louis, MO). Methanol (Optima LC/MS grade) was purchased from Thermo Fisher Scientific (Scoresby, Australia). Compressed helium (ultrahigh purity, 99.999%) was obtained from Coregas (Sydney, Australia). All commercial compounds were used as received without further purification.

Instrumentation

Gas-phase ion-molecule experiments were performed on a modified [25, 26] linear quadrupole ion trap mass spectrometer (LTQ XL, Thermo Fisher Scientific, San Jose, CA) operating Xcalibur version 3.0 software and equipped with a heated electrospray ionization (HESI) source. The HESI source was connected to both the instrument syringe pump and an HPLC system (Dionex UltiMate 3000 RSLC, Thermo Fisher Scientific, San Jose CA) via a tee union. Methanol or acetonitrile solutions containing 5 – 10 μM of individual radical precursors were tee-infused at a rate of 5 – 10 μL min^{-1} into an HPLC flow of 100% methanol or acetonitrile (50 – 100 μL min^{-1}) that eluted into the source. Typical source conditions for negative ion mode were: capillary temperature: 250 °C, source heater temperature: 250 °C, sheath gas flow rate: 25 – 30 arbitrary units, auxiliary and sweep gas flow rates: 0 – 5 arbitrary units, spray voltage: -3.5 – 4 kV, capillary voltage: -35 – 40 V, tube lens: -45 – 50 V. Typical source conditions for positive ion mode were: capillary temperature: 250 °C, source heater temperature: 50 °C, sheath gas flow rate: 25 – 30 arbitrary units, auxiliary and sweep gas

flow rates: 0 – 5 arbitrary units, spray voltage: 4 – 4.5 kV, capillary voltage: 10 – 20 V, tube lens: 35 – 45 V. For collision-induced dissociation experiments, ions were mass-selected with an isolation width of 1.5 – 2.0 Th, using an activation q-parameter of 0.250. The normalized collision energy applied was typically 25 – 30 arbitrary units with an excitation time of 30 ms (unless otherwise specified).

Previous work by ourselves and others has indicated that synthesis of distonic radical ions by photodissociation can give greater regioselectivity than collision-induced dissociation [5, 27]. To facilitate photodissociation of trapped ions instrument modifications that allow laser irradiation of ions confined within the linear ion trap are similar to those reported by Ly and Julian and have been described in detail elsewhere [12, 28]. Briefly, the posterior plate of the mass spectrometer was modified with a quartz window to transmit the fourth-harmonic (266 nm) of a Nd:YAG laser (Continuum, Santa Clara, CA). The window was positioned on the backplate to direct laser access to the ions within the ion trap through the 2 mm aperture centered on the back lens. Laser pulses were aligned through the aperture in the back lens by two right-angle steering prisms, adjusted to optimize beam overlap with the ion cloud (see Figure S-1, Supporting Information). Laser pulses were synchronized to the beginning of an MS^2 ion activation step with a TTL trigger signal generated by the mass spectrometer to the laser *via* a digital delay generator [29]. In these photodissociation experiments, the normalized collision energy was set to 0 (arbitrary units) such that all product ions arise from excitation by the laser pulse. Only a single laser pulse irradiates the target ions in each MS cycle.

Instrument modifications that allow for neutral reagent molecules to be seeded into the ion trap region of the instrument are similar to those previously described [15, 25]. Briefly, the native helium splitter was bypassed in order to directly connect an external reagent mixing manifold to the ion trap (see Figure S-1, Supporting Information). Helium flow to the ion trap was controlled by a variable leak valve (Granville-Phillips Model 203, Boulder, CO) providing a pressure reading of 0.8 x 10^{-5} Torr on the instrument ion gauge. Neutral reagents,

such as dimethyldisulfide, were introduced by placing a droplet of liquid into the end-cap of a stainless steel Swagelok cap and placing under vacuum before opening the line to the manifold. The flow of reagent was controlled by a PEEKsil restriction (100 mm length, internal diameter 25 μm). For observing reactions with dioxygen, no reagent was added and adventitious background air within the instrument provided a concentration of dioxygen that was sufficient for the experiments.

Ion-molecule kinetics

Pseudo first-order rate constants, k_1 (s^{-1}), were obtained by recording a series of mass spectra as a function of storage time for the reaction between the radical ion and neutral reagent. Each spectrum recorded was an average of at least 60 individual spectra. The reaction time was defined as the interval between the isolation of the selected radical ion and ejection of all ions from the trap for detection. Reaction times of 50 – 6000 ms were set using the activation time parameter within the instrument control software. A plot of the mean radical ion abundance against reaction time yielded a single exponential relationship. Fitting the data to Equation 1 gave the pseudo-first order rate constant for the reaction, k_1 (s^{-1}). Second-order rate constants, k_2 (cm^3 molecule^{-1} s^{-1}), were obtained from k_1 and the concentration of dioxygen ([O$_2$]) present in the ion trap region of the mass spectrometer (Equation 2) [30] where [O$_2$] was determined from the calibration reaction of 3-carboxylatoadamantyl radical anion with dioxygen under the same instrumental conditions [25]. Reaction efficiencies, Φ, (*i.e.,* the percentage of ion-molecule collisions that resulted in product formation) were determined according to Equation 3, where the collision rate constant, k_{coll}, is determined by average dipole orientation (ADO) theory at 307 K [31]. The temperature of ions stored within a linear quadrupole ion trap has been estimated at 318 ± 23 K [32], consistent with an earlier estimate of 307 ± 1 K [25], which can be taken as the effective temperature for ion-molecule reactions observed herein [33, 34]. While the accuracy

of the rate constant measurements is estimated to be $\pm$ 50%, the precision of the measurements is better than $\pm 10\%$.

$$[R^\bullet]_t = [R^\bullet]_0 e^{-k_1 t} \qquad \text{(Eqn. 1)}$$

$$k_2 = \frac{-k_1}{[O_2]} \qquad \text{(Eqn. 2)}$$

$$\Phi = \frac{k_2}{k_{coll}} * 100 \qquad \text{(Eqn. 3)}$$

Computational methods

The Gaussian 09 suite of programs was used for all computations [35]. Electronic energies and thermally corrected (298 K) enthalpies for all ground-state species were computed using the hybrid meta-GAA M06-2X functional [36, 37] and the 6-311++G(d,p) basis set. DFT calculations for doublet states employed an unrestricted formalism. This computational strategy has previously been shown to be effective in modelling the thermochemical and spectroscopic properties of gas phase arylperoxyl radicals [23]. All stationary points on the potential energy surface were verified to be either local minima (no imaginary frequencies) or transition states (one imaginary frequency) by computation of analytic vibrational frequencies. Transition states were connected to minima by calculation of the intrinsic reaction coordinate (IRC). Outputs from all calculations discussed in this study are summarized in the Supporting Information.

Results and Discussion

Formation of charge-tagged phenyl radicals in the gas phase

Aryl iodide precursor ions were generated by electrospray ionization (in either positive or negative ion mode), mass selected and subsequently irradiated at 266 nm within the ion trap mass spectrometer to liberate the distonic radical ions **1 – 7** (Chart 1). Photodissociation of aryl iodides has been demonstrated as an effective means of generating aryl radicals with high regiospecificity and the approach has been deployed to great effect by Julian and co-workers for molecular structure elucidation *via* radical-directed dissociation [28, 38]. In this study, the putative structure of the radical ions was confirmed for each instance by observing the gas phase reaction with dimethyl disulphide [11, 25, 39-41]. For all radical ions **1 – 7** the reaction resulted in thiomethyl abstraction consistent with the distonic radical ion structures shown in Chart 1 (see example spectrum in Figure S-2, Supporting Information).

Charge polarity effect on products of phenyl radical reactions

Both *para-* and *meta-*(*N,N,N*-trimethylammonium)phenyl radical cations (**1** and **2**) were prepared by 266 nm photodissociation of mass-selected 4- and 3-iodo-*N,N,N*-trimethylanilinium cations, respectively. Mass-selection and isolation of *m/z* 135 within the ion trap allowed for observation of the reactions of the radical cations **1** and **2** with background oxygen at timescales ranging from 100 – 10,000 ms. These observations revealed that reaction of **1** and **2** with O_2 predominantly resulted in the formation of phenylperoxyl radical cations (*m/z* 167) **1-OO** and **2-OO,** respectively (Figure 1). Two trace product ions of *m/z* 151 and *m/z* 138 were also observed arising from the peroxyl radicals (see 50x magnification in Figure 1). Decomposition of **1-OO** and **2-OO** by cleavage of the O–O bond results in the loss of an O (^{3}P) atom, ultimately forming *p-* and *m-*(*N,N,N*-trimethylammonium)phenoxyl radical cations of *m/z* 151. The product ion of *m/z* 138 corresponds to the loss of a formyl radical (-HCO, -27 Da) from the peroxyl radical intermediate to form a charge-labeled cyclopentadienone. These observations are consistent

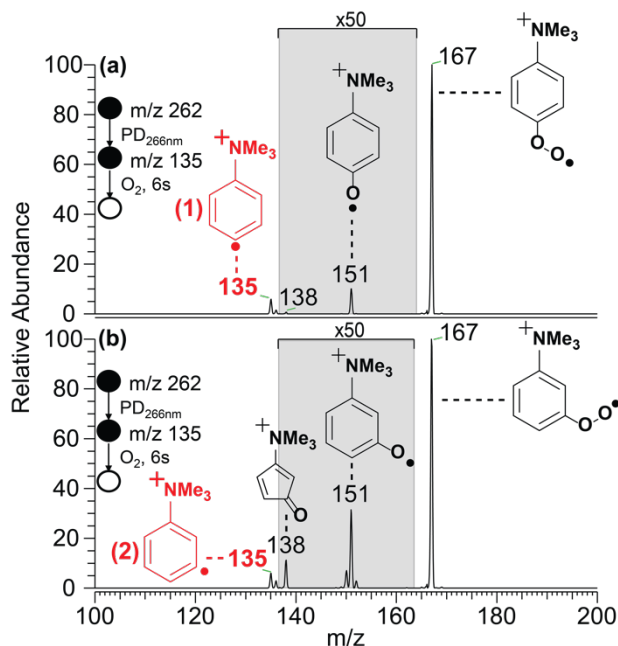with our previous exploration of the reaction of positively charged arylperoxyl radicals with dioxygen [15].

Figure 1. (a) Mass spectrum arising following the reaction of 4-(*N,N,N*-trimethylammonium)phenyl radical cation, *m/z* 135 (**1**), with O_2 for 6 s. (b) Mass spectrum arising following the reaction of 3-(*N,N,N*,-trimethylammonium)phenyl radical cation, *m/z* 135 (**2**), with O_2 for 6 s . Trace amounts of hydrogen atom abstraction by **1** and **2** from a small amount of contaminant present in the mixing manifold was also observed.

The reactivity of the *p*- and *m*-trifluoroboratophenyl radical anions, **3** and **4** respectively, toward O_2 are reported here for the first time. The spectra shown in Figure 2 reveal that the reaction produces only trace amounts of the peroxyl radical adduct with ions corresponding to **3-OO** and **4-OO** (*m/z* 176) observable only at 50x magnification (Figure 2). Numerous product ions consistent with the facile decomposition of these $[M+O_2]^{\bullet-}$ adduct ions are observed, pointing to the fleeting lifetime of the arylperoxyl radicals formed in both cases. Scheme 1 presents the possible rearrangement and decomposition pathways available to the peroxyl radical **4-OO** and is based upon a previous computational investigation of the potential energy surface for the analogous 4-carboxylatophenyl peroxyl radical anion, **5-OO** [15]. The major product ions in the spectra in Figure 2 are observed at *m/z* 147 corresponding to $[M+O_2-CHO]^-$ arising from ejection of a formyl radical from the peroxyl radical intermediate (Scheme 1 for **4-OO**, for analogous **3-OO** see Scheme S-1 Supporting Information). The spectra also reveal a minor product ion at *m/z* 175 that could

be rationalized as a charge-tagged benzoquinone anion arising from the loss of atomic hydrogen. *o*-Benzoquinones are known to eject carbon monoxide to yield cyclopentadienones [42, 43], hence prompt loss of CO from the *m/z* 175 anion population may also contribute to the abundant product ion signal observed at *m/z* 147 (Scheme 1). Other major phenylperoxyl radical decomposition products observed arise from cleavage of the oxygen-oxygen bond in the peroxyl radical to form a phenoxyl radical anion (*m/z* 160), as well as ejection of the BF_3 charge tag to form $[M+O_2-BF_3]^{\bullet-}$ ions at *m/z* 108. The abundant loss of BF_3 from **3-OO** and **4-OO** (*m/z* 108) is rather surprising. Calculations predict that direct ejection of BF_3 from **3-OO** to form a peroxyl phenide radical anion is 26.2 kcal mol^{-1} above the entrance channel (data not shown). Hence, the loss of BF_3 most likely arises from isomerization followed by migration of an oxygen atom around the aromatic ring of **3-OO** and **4-OO** to form *p*- and *m*-benzoquinone radical anions (Scheme 1). Lastly, minor decomposition product ions of *m/z* 119 were also observed presumably arising from decarbonylation of cyclopentadienone intermediates (*m/z* 147) to form charge-tagged cyclopentadienone or vinylacetylene anions (Scheme 1). These observations are consistent with recent temperature-dependent studies examining the pyrolysis of cyclopentadienone that have found that vinylacetylene production dominates at lower temperatures (1000 – 1400 K) [44]. Reactivity of the *p*- and *m*-carboxylatophenyl radical anions (**5** and **6** respectively), toward O_2 was also examined and the corresponding spectra are shown in Figure S-3 (Supporting Information). The observed reaction products are consistent with previous reports and are analogous to the channels observed for the trifluoroborates, **3** and **4**.
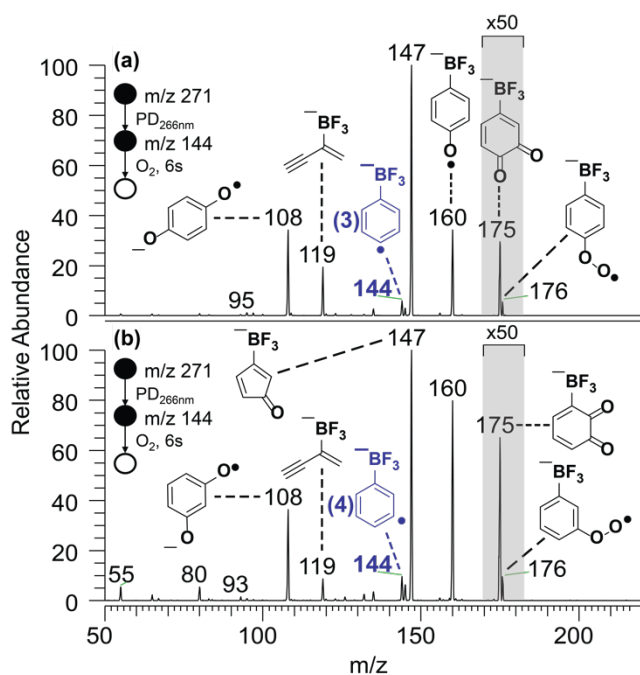
Figure 2. (a) Mass spectrum arising from the reaction of 4-(trifluoroboronato)phenyl radical anion, *m/z* 144 (**3**), with O$_2$ for 6 s. (b) Mass spectrum arising from the reaction of 3-(trifluoroboronato)phenyl radical anion, *m/z* 144 (**4**), with O$_2$ for 6 s. Trace amounts of hydrogen atom abstraction by **3** and **4** from a small amount of contaminant present in the mixing manifold was also observed.
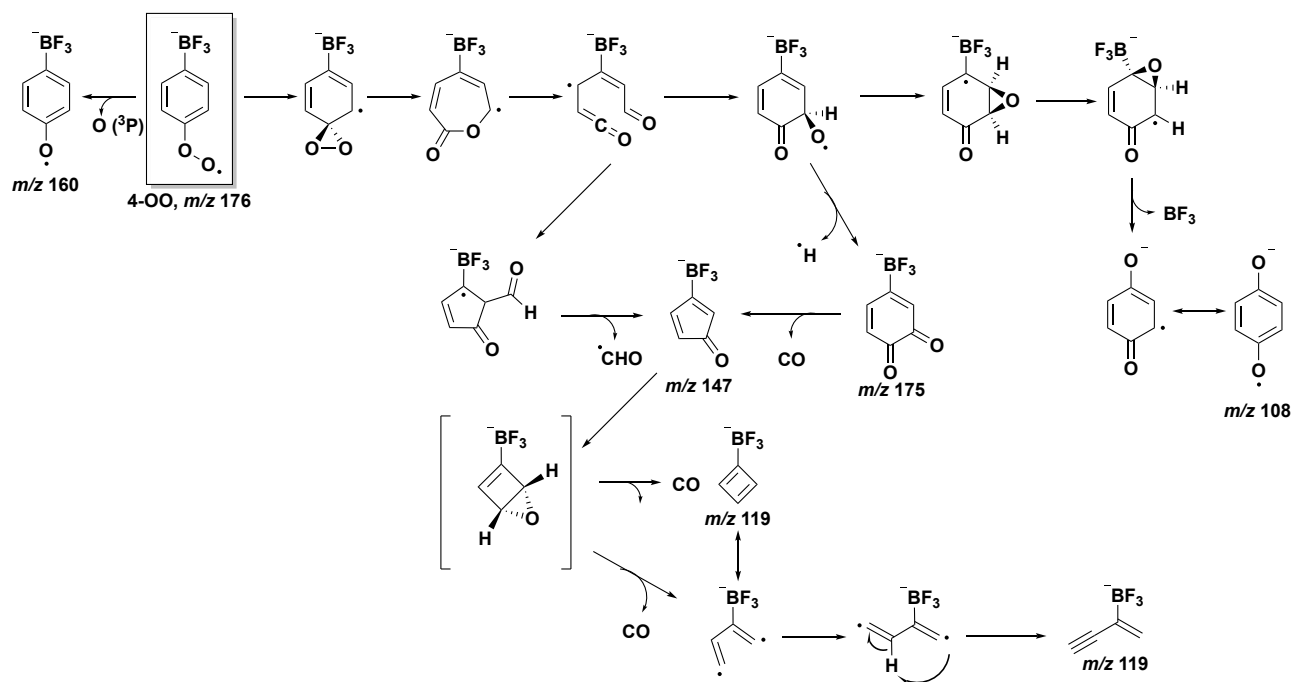
Scheme 1

Charge polarity effect on the reaction potential energy surface

The stark difference between the oxidation product distributions of positive and negative charge-tagged phenyl radicals suggests significant modulation of the potential energy surface between the two systems. To assist in rationalizing these experimental

13

observations and to enable comparison to the neutral phenyl radical archetype, the reaction enthalpies ($\Delta_{rxn}H_{298}$) of selected intermediates and transition states for the neutral and charge-tagged phenyl radical plus dioxygen systems were calculated at the (U)M06-2X/6-311++G(d,p) level of theory (Figure 3). A substantial body of theoretical investigations on the phenylperoxyl radical potential energy surface have concluded that isomerization by addition of the peroxyl radical oxygen back onto the *ipso*-carbon of the aromatic ring to form a dioxiranyl intermediate is the lowest energy isomerization pathway (**N4**, Figure 3) [15, 16, 45-51]. This dioxiranyl radical, along with the phenoxyl radical arising from oxygen-oxygen bond homolysis, thus represent the key reaction intermediates leading to the formation of all product ions (see above) and hence the influence of the charged moieties on these reaction steps have been examined computationally.
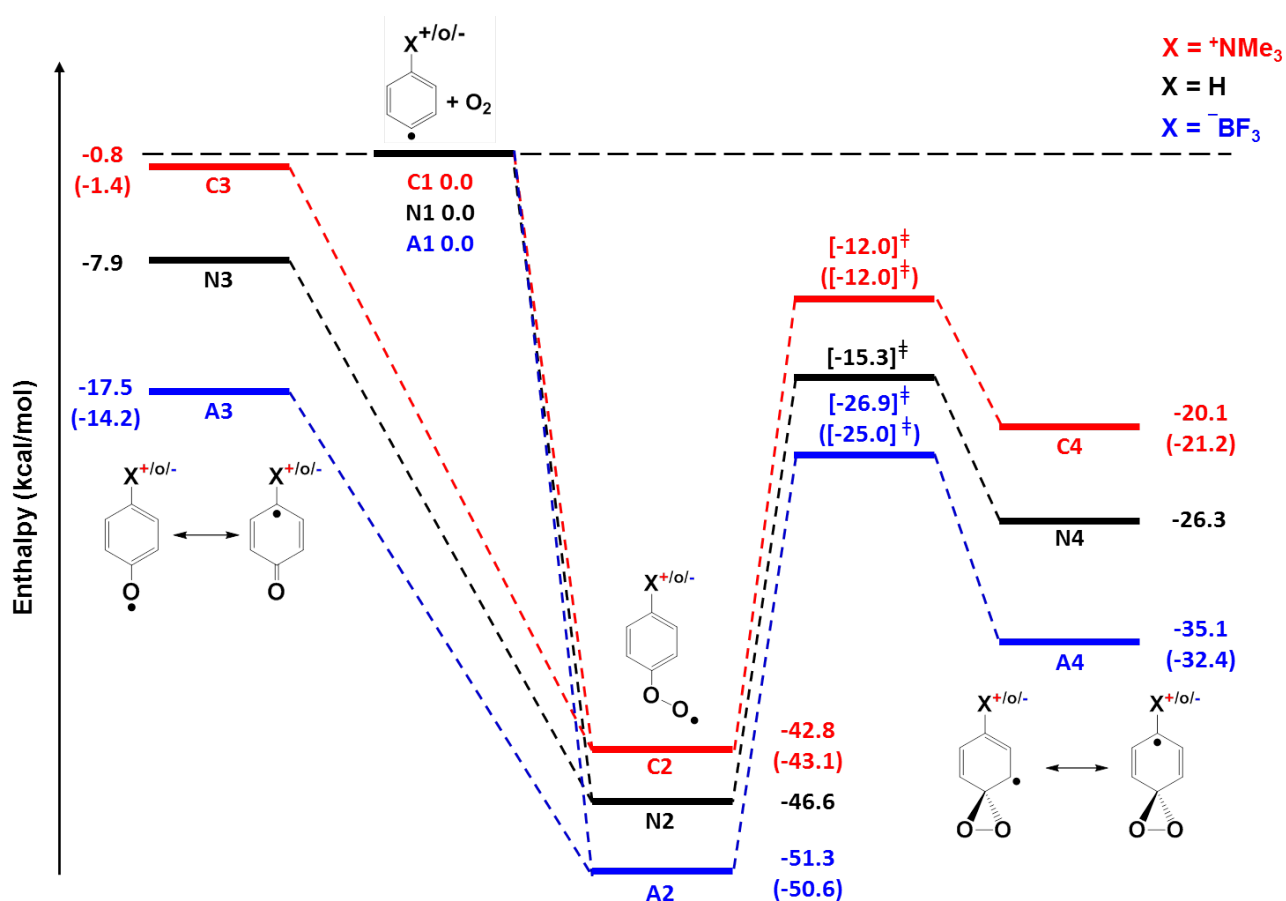

Figure 3. Potential energy surface of the positive (red, X = NMe$_3$$^+$) and negative (blue, X = BF$_3$$^-$) charge-tagged and neutral (black, X = H) Ph$^•$ + O$_2$ reactions for comparison of the formation of phenoxyl radical and phenyldioxiranyl radical intermediates leading to further phenylperoxyl radical decomposition. Calculated at the (U)M06-2X/6-311++G(d,p) level. Energies for the *meta*-substituted analogues are shown in parentheses.

The computational results, summarised in Figure 3, illustrate that addition of O_2 to the neutral phenyl radical produces the phenylperoxyl radical (**N2**) with an exothermicity of 46.6 kcal mol^{-1}. Homolytic cleavage of the O–O bond in **N2** yields the phenoxyl radical plus atomic oxygen (^3P) (**N3**) that is 7.9 kcal mol^{-1} below **N1**. Alternatively, the oxygen-centered radical of the peroxyl moiety in **N2** can undergo addition to the *ipso*-carbon of the aromatic ring forming the dioxiranyl intermediate (**N4**) that is 26.3 kcal mol^{-1} below the entrance channel on the neutral surface. This isomerization occurs through the transition state **TS N2 → N4** that represents a barrier of 31.3 kcal mol^{-1} with respect to the phenylperoxyl radical (**N2**) but is still some 15.3 kcal mol^{-1} below **N1**.

In the presence of the positively charged trimethylammonium moiety at the *para*-position, the addition of dioxygen to the phenyl radical cation (**C2**) is exothermic by 42.8 kcal mol^{-1} (Figure 3 red lines). Interestingly on the cation surface, the minimum for the phenylperoxyl radical **C2** lies in a well that is 3.8 kcal mol^{-1} shallower than the comparable neutral peroxyl radical (**N2**). The *p*-(*N,N,N*-trimethylammonium)phenoxyl radical (**C3**) formed upon homolysis of the O–O bond in **C2** is 7.1 kcal mol^{-1} higher in energy than the neutral phenoxyl radical and lies just 0.8 kcal mol^{-1} below the entrance channel (**C1**). Similarly, the transition state **TS C2 → C4** is predicted to lie 12.0 kcal mol^{-1} below **C1** which is 3.8 kcal mol^{-1} above the comparable barrier on the neutral surface (**TS N2 → N4**). Furthermore, the dioxiranyl intermediate **C4** is also predicted to be 6.2 kcal mol^{-1} higher in energy than the neutral archetype **N4**; lying 20.1 kcal mol^{-1} below **C1**. Interestingly, when the fixed positive charge-tag is substituted at the *meta*-position with respect to the radical site, the destabilizing effect of the charge-tag does not vary significantly from the *para*-substituted isomer (*cf.* values in parentheses in Figure 3). This finding indicates that the difference between the positively-charged and neutral phenyl radical potential energy surfaces is not strongly influenced by formal charge or radical delocalisation around the aromatic ring.

Considering the negatively charged analogue, addition of dioxygen to the *p*-trifluoroboratophenyl radical anion forms the *p*-trifluoroboratophenylperoxyl radical anion

(**A2**) which resides in a minimum some 51.3 kcal mol^{-1} below the entrance channel (**A1**, Figure 3). When normalised to the energy of the entrance channel, the negatively-charged peroxyl radical is 4.7 kcal mol^{-1} below its neutral counterpart **N2**. Comparison to the corresponding cation **C2** reveals that the stabilization of the peroxyl radical by the proximate negative charge is larger in magnitude than the destabilisation in the cation (*cf.* 3.8 kcal mol^{-1}). The *p*-trifluoroboratophenoxyl radical anion (**A3**) formed upon cleavage of the O–O bond in **A2** is predicted to be 9.6 kcal mol^{-1} lower in energy than **N3**, lying 17.5 kcal mol^{-1} below **A1**. The barrier to isomerization of **A2** to form the dioxiranyl intermediate **A4** is predicted to be 24.7 kcal mol^{-1} (**TS A2 → A4**) and is thus 4.7 kcal mol^{-1} lower in energy than the equivalent neutral transition state **TS N2 → N4**. **A4** is computed to be 8.8 kcal mol^{-1} lower in energy than **N4**, lying 35.1 kcal mol^{-1} below the entrance channel. The net lowering of the potential energy surface relative to the entrance channel is also observed when the fixed negative charge-tag is in the *meta*-position with respect to the radical site (values in parentheses in Figure 3), indicating that resonance effects are only minor contributors to the overall stabilization afforded by the anion moiety.

The normalized reaction coordinate diagrams of the positively and negatively charge-tagged phenyl radicals in Figure 3 give some insight into the differences in experimentally observed reaction products for the two polarities (*vide supra*). For example, in the positively charge-tagged system the barriers to direct decomposition or rearrangement of the intermediate peroxyl radicals **1-OO** and **2-OO** lie much closer to the entrance channel (*cf.* red lines in Figure 3). These findings suggest that the rate of decomposition will be significantly slower than for the corresponding anions or neutrals and affording a greater contribution from stabilization of the peroxyl adduct. This is consistent with the observation of phenylperoxyl radical formation (*i.e.*, **1-OO** and **2-OO**) as the predominant reaction product with only trace amounts of the [M+O$_2$-O]$^{\bullet+}$ and [M+O$_2$-CHO]$^{\bullet+}$ decomposition products (see Figure 1). Conversely, for the negative ions the transition states and intermediates in the decomposition pathways are lowered substantially relative to both the cation and neutral

analogues (*cf*. blue lines in Figure 3). These calculations are thus consistent with higher rates for unimolecular transformation of the intermediate peroxyl radicals **3-OO** and **4-OO** to decomposition products. Such rapid transformations could outcompete stabilisation of the adduct ions and explain why only trace amounts of the **3-OO** and **4-OO** anions are observed experimentally (Figure 2). The computational results illustrated in Figure 3 suggest that the distonic ion reactivity observed in this study is likely to bracket that of the neutral phenyl radicals. It would be interesting therefore, to assess whether increasing the distance between charged and radical moieties might allow convergence (from above and below) on the energetics of the neutral phenyl radical archetype.

Charge-radical distance effects on the reaction potential energy surface

The effect of the intramolecular separation of charged and radical moieties was investigated computationally for the phenyl radical plus dioxygen reaction. The approach used in this study follows the strategy devised by Grob et al. [52] that has been recently been deployed in probing energetic and spectroscopic shifts associated with charge-radical separation in distonic ions [16, 21, 23]. Here, the reaction enthalpies for selected stationary points on the Ph$^\bullet$ + O$_2$ potential energy surface were computed for a series of *para*-substituted phenyl radicals of the form X-(CH$_2$)$_n$-Ph$^\bullet$ (where X = $^-$BF$_3$ or (CH$_3$)$_3$N$^+$ and *n* = 1 - 7). Comparing the enthalpy of each stationary point - relative to the entrance channel - with the analogous $\Delta_{rxn}H$ values derived from neutrals of the form X-(CH$_2$)$_n$-Ph$^\bullet$ (where X = H) gives a stabilization or destabilization enthalpy ($\Delta\Delta_{rxn}H$) resulting from the charge at a distance defined by the number of methylene groups (*n*) separating the charge carrier from the phenyl ring. In these calculations, the extended hydrocarbon chain was deliberately constrained to an all gauche conformation so as to extend, as far as possible, the distance between the charge and radical sites for a given number of methylene units. Figure 4 plots the $\Delta\Delta_{rxn}H$ values computed (relative to the corresponding neutral radical, indicated as a dashed horizontal line) for (a) the phenylperoxyl radical intermediate (X-(CH$_2$)$_n$-PhOO$^\bullet$) (b)

the phenoxyl radical exit channel (X-(CH$_2$)$_n$-PhO$^\bullet$) and (c) the dioxiranyl intermediate. The enthalpy differences are plotted against the reciprocal distance (1/r) between the boron or nitrogen (for X = $^-$BF$_3$ or (CH$_3$)$_3$N$^+$, respectively) and the radical centre which is taken as the terminal oxygen atom of the peroxyl radical (Figure 4a) or the *para*-carbon of the phenyl ring for the phenoxyl and dioxiranyl structures as illustrated in Figures 4(b) and (c), respectively.
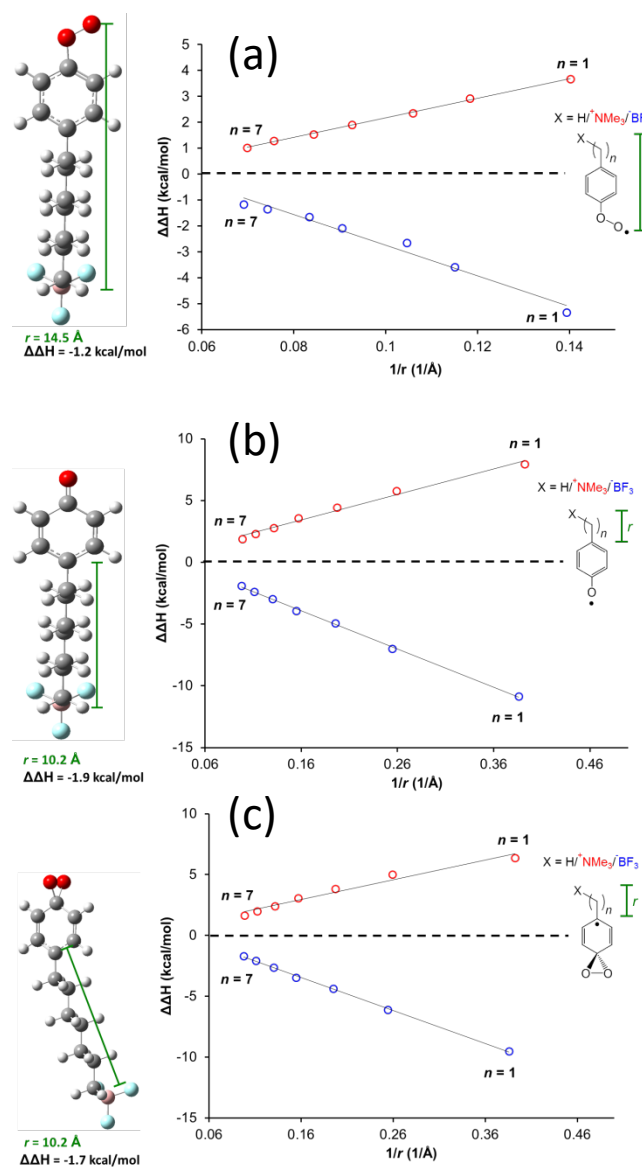

Figure 4. Stationary point enthalpies relative to the entrance channel for the X-(CH$_2$)$_n$-Ph$^\bullet$ + O$_2$ potential energy surfaces (where X = $^-$BF$_3$ (blue circles) or (CH$_3$)$_3$N$^+$ (red circles) and n = 1 – 7) are plotted as a difference in enthalpy to the corresponding stationary points on the neutral potential energy surface for the H-(CH$_2$)$_n$-Ph$^\bullet$ + O$_2$ reaction. Enthalpy differences (at 298 K) were computed at the (U)M06-2X/6-311++G(d,p) level of theory and are plotted (in kcal mol^{-1}) against reciprocal distance between the charge an radical moieties as indicated by the green lines on the representative structures shown. Enthalpy differences are shown for (a) the phenylperoxyl radical (where y[(CH$_3$)$_3$N$^+$] = 37.777x - 1.6043, R^2 = 0.99814 and y[$^-$BF$_3$] = -59.089x + 3.1586, R^2 = 0.97784); (b) the phenoxyl radical (where y[(CH$_3$)$_3$N$^+$] = 20.592x - 0.1393, R^2 = 0.98642 and y[$^-$BF$_3$] = -30.923x + 1.0263, R^2 = 0.99886) and (c) the dioxiranyl intermediate (where y[(CH$_3$)$_3$N$^+$] = 16.28x - 0.3357, R^2 = 0.96722 and y[$^-$BF$_3$] = -27.167x + 0.8888, R^2 = 0.99902). Representative structures for all three reaction intermediates and products are provided.

The stabilization of the phenylperoxyl radical computed for a remote, fixed negative charge and the destabilization of the phenylperoxyl radical afforded by a remote, fixed positive charge were both found to decay linearly with $1/r$ (Figure 4a). The same was found to be true for the phenoxyl radical and dioxiranyl radical intermediates (Figures 5b and c). Interestingly, the enthalpy perturbations arising from a remote, fixed-charge moiety on the reaction intermediates in the Ph$^{\bullet}$ + O$_2$ reaction manifold are persistent over long intra-molecular distances. For example, a (de)stabilization of the phenylperoxyl radical by ~1 kcal mol^{-1} is calculated even when the charge-radical separation is 14.5 Å (Figure 4a) and a similar (de)stabilization the phenoxyl radicals and dioxiranyl radical intermediates by ~2 kcal mol^{-1} over distances of 10.2 Å (Figures 5b and c). The linear fits of these data predict that convergence of the positively and negatively charged distonic radical ions could be expected at charge-radical distances of up to 19 Å. Testing this prediction experimentally however, presents a challenge in identifying a suitable molecular scaffold capable of maintaining a rigid separation over such distances between a well-defined charged group and an unpaired electron. Nonetheless the calculations presented in Figure 4 also suggest that a modest increase in charge-radical separation of just 2.4 Å (n = 3) could reduce the stabilizing effect of the negative charge by a factor of 2, and reduce the destabilizing effect of the positive charge by a factor of 1.5. This might suggest, for example, that a rigidly imposed charge-radical separation of 9 - 10 Å in a negatively charge-tagged phenyl radical may be enough to slow the decomposition and rearrangement reactions of the peroxyl radical intermediate and thus measurably alter the product distribution of the Ph$^{\bullet}$ + O$_2$ reaction.

To experimentally test the effect of charge-radical separation on the products of arylperoxyl forming reactions, the reaction of the 4-(1-carboxylatoadamantyl)phenyl radical anion (**7**) with dioxygen was investigated in the ion trap mass spectrometer and compared side-by-side with the reactions of the 4-carboxylatophenyl radical (**5**). Molecular orbital calculations estimate the distance between the radical site and the charged moiety in **7** is 9.1 Å, representing an increase in separation of 5.3 Å compared with **5** (data not shown). Figure

5(a) and (b) show the mass spectra obtained after isolation of the radical anions **5** and **7**, respectively, in the presence of dioxygen for 5 s. The spectrum obtained from 4-carboxylatophenyl radical anion (*m/z* 120) is dominated by the phenoxyl radical product ion at *m/z* 136 with the corresponding phenylperoxyl radical (**5-OO**) at *m/z* 152 only present at very low abundance (see 40x magnification in Figure 5a). In contrast, analogous reaction of the 4-(1-carboxylatoadamantyl)phenyl radical anion (*m/z* 254) with O_2 yields an abundant **7-OO** product ion at *m/z* 286 (Figure 5b) with the phenoxyl radical plus atomic oxygen product channel (*m/z* 270) making a significantly diminished contribution (see 40x magnification in Figure 5a). These observations are consistent with the computational predictions (*vide supra*) that increasing the charge-radical separation raises the barriers toward decomposition and isomerization of the phenylperoxyl radical, thus providing a greater opportunity for stabilization of adduct ion.
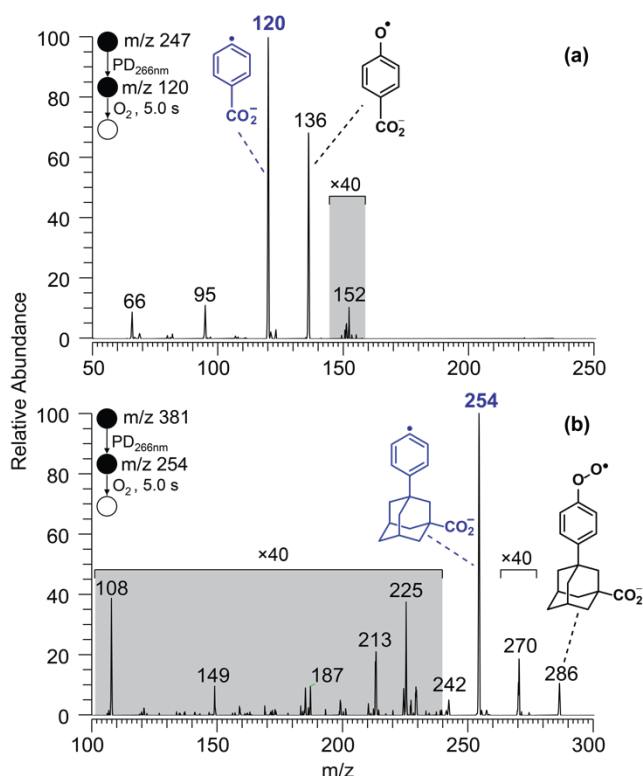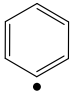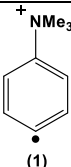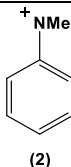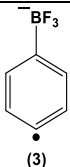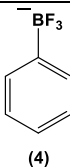

Figure 5. Mass spectra resulting from the reaction of (a) the 4-carboxylatophenyl radical anion, *m/z* 120 (**5**), and (b) the 4-(1-carboxylatoadamantyl)phenyl radical anion, *m/z* 254 (**7**), with dioxygen for 5 s.

Charge polarity and charge-radical distance effects on the rate of phenyl radical reactions

The second-order rate constants for the reaction of charge-tagged phenyl radicals **1 - 4** with dioxygen were derived from measured pseudo-first order rate constants and are

reported in Table 1. These rate constants range from k_2 = 3.6 – 6.7 x 10^{-11} cm^3 $molecule^{-1}$ s^{-1} and are 3 – 5 times greater than the comparable rates measured for the neutral phenyl radical previously reported (Table 1) [53-55]. In order to normalize for the effect of charge on collision dynamics, the reaction efficiencies were determined through estimation of the collision rate for the different reactions (Table 1). Using an estimated hard sphere collision rate of 3.2 x 10^{-10} cm^3 $molecule^{-1}$ s^{-1}, the reaction efficiency for the neutral phenyl radical with dioxygen was estimated to range between 4 – 6%. In comparison, efficiencies for the reactions of **1** – **4** ranged from 6 – 12%. Contrasting the two polarities, the presence of the negative charge leads to a significantly higher reaction efficiency (Φ = 10 and 12%, for **3** and **4**, respectively) compared with the positively charged analogues that are much closer to the neutral archetype (Φ = 6 and 7%, for **1** and **2**, respectively). Noting that the relative uncertainty in the efficiency determinations is considerably smaller than the absolute uncertainty listed in Table 1, radicals **2** and **4** react slightly faster than their *para*-substituted isomers **1** and **3**, respectively. As well as the position of the charged moiety on the benzene ring, the effect on reaction efficiency of intramolecular charge-radical separation was also explored. The reaction efficiencies of the 4-carboxylatophenyl radical anion (**5**) and the 4-(1-carboxylatoadamantyl)phenyl radical anion (**7**) were measured to be 8 (±1) % and 6 (±1) %, respectively. This result suggests that removing the negatively charged moiety further from the phenyl radical center retards the reaction efficiency bringing it closer to the reactivity of the cations **1** and **2** and current estimates of the neutral phenyl radical.

Table 1. Comparison of 2nd order rate constant and reaction efficiencies for the ion-molecule reactions of distonic radical ions **1 – 4** with O$_2$. We estimate the absolute uncertainty in the rate constants to be 50%.

Radical		$^+$NMe$_3$ (1)	$^+$NMe$_3$ (2)	$^-$BF$_3$ (3)	$^-$BF$_3$ (4)
Rate constant k_2 **(cm^{3}molecule^{-1} s^{-1})**	1.8 ± 0.1 x 10$^{-11 a}$ 1.4 ± 0.4 x 10$^{-11 b}$ 1.2 ± 0.1 x 10$^{-11 c}$	3.6 ± 0.6 x 10^{-11}	3.9 ± 0.4 x 10^{-11}	5.6 ± 0.7 x 10^{-11}	6.7 ± 1.2 x 10^{-11}
Collision rate k_{coll} **(cm^{3}molecule^{-1} s^{-1})**	3.2 x 10$^{-10 d}$	5.79 x 10^{-10}	5.79 x 10^{-10}	5.76 x 10^{-10}	5.76 x 10^{-10}
Reaction Efficiency (k_2/ k_{coll} **× 100%**)	6 % 4 % 4 %	6 ± 1 %	7 ± 1 %	10 ± 1 %	12 ± 1 %

[a] Value from Reference [53]. [b] Value from Reference [54]. [c] Value from Reference [55]. [d] Hard sphere collision rate estimated using $k_{hs} = \pi \sigma_{AB}^2 \left(\frac{8k_B T}{\pi \mu} \right)^{1/2}$, where $\sigma_{AB}^2 = (R_A + R_B)^2$.

The reaction efficiency results summarised in Table 1 are interesting to juxtapose against the potential energy surfaces summarised in Figure 3. The computational results in Figure 3 suggest that all Ph$^•$ + O$_2$ reactions should proceed by the barrierless recombination of the phenyl radical with dioxygen. Such a barrierless and highly exothermic reaction ($\Delta_{rxn}H$ = -42.4 – -51.9 kcal mol^{-1}) might be expected to have an efficiency near unity (*i.e.*,100%). In contrast, the experimental findings resented here indicate reaction efficiencies of <12 % in all instances and, moreover, that the efficiencies are modulated by the polarity, location and distance between the radical and charged moieties. These findings perhaps point to a more nuanced potential energy surface with both a shallow pre-reactive complex and reef-type barrier just below the entrance channel that represent the rate-determining step in the recombination reaction. Investigation of this extremely flat portion of the potential energy surface using electronic structure calculations is challenging and beyond the scope of the current study. Computational studies of related gas phase ion-molecule reactions however, have served to highlighted the importance of the potential energy landscape surrounding the entrance channel in modulating the reaction kinetics [56, 57]. As indicated in the hypothetical surface in Figure 6, we can conclude based on the experimental findings that - relative to the

entrance channel - the barrier to reaction will be lowered in the presence of an anion while the cations have much less impact on the barrier height. Future experiments and high-level calculations will provide insights into the nature of this barrier and its role in dictating reaction rate in arylperoxyl forming reactions.
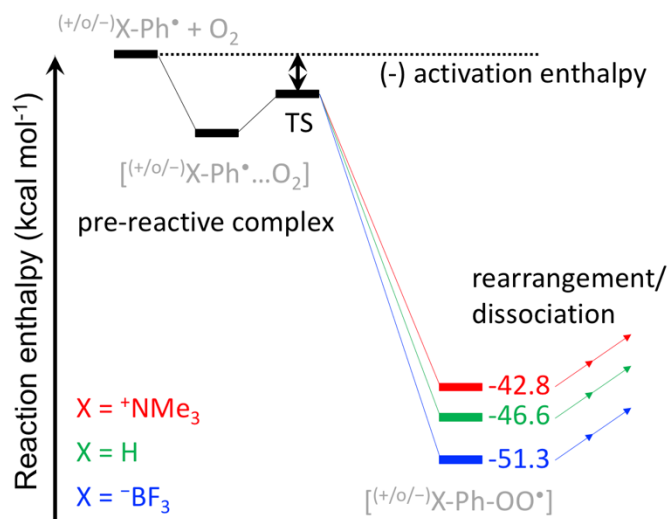

Figure 6. Hypothetical potential energy surface for the formation of a pre-reactive complex upon radical combination of Ph[•] and O_2 giving rise to a small barrier to phenylperoxyl radical formation.

Conclusions

Through a combined experimental and computational examination, we have demonstrated that the polarity of the charge-tag significantly perturbs the potential energy surface of the Ph$^\bullet$ + O$_2$ reaction system; altering both the reaction kinetics as well as the reaction products observed. The presence of a fixed-positive charge was found to destabilize influential stationary points on the Ph$^\bullet$ + O$_2$ potential energy surface relative to the entrance channel. In contrast, a fixed-negative charge was found to lower the energy of the same stationary points on the corresponding anionic potential energy surface. The opposite but unequal perturbation arising from these charge-tags can account for the different product distributions of the Ph$^\bullet$ + O$_2$ reaction and also the measured differences in reaction efficiency. Computational exploration of these effects with increasing intra-molecular separation of charge and radical sites suggests that, in the gas phase, the charge can influence the energetics associated with the formation and fate of peroxyl radicals over surprisingly long distances (*e.g.*, up to 14.5 Å). These predictions were supported by experimental examination of the reactivity of the 4-(1-carboxylatoadamantyl)phenyl radical anion (**7**), where the molecular structure imposes a charge-radical separation of 9.1 Å. Increasing the charge-radical separation in this system was shown to retard the reaction efficiency and significantly alter the product distribution in favour of the phenylperoxyl radicals. The demonstrated influence of remote charges in modulating peroxyl-forming reactions may have broader implications [21, 22]. In a biological context for example, the presence of remote charged moieties may afford switching of peroxyl radical reactivity in enzymatic or free radical-induced oxidation chemistries. While the effective range of influence of charge-radical polarization would be diminished in polar solvents, in low polarity regimes such as hydrophobic pockets of proteins or membrane bilayers the effect could be comparable to that observed in the gas phase.

Acknowledgements

Supporting Information

Additional experimental details, mass spectra and computational archive data are provided as supporting information. An archive of the raw data files used to create some of the figures in this manuscript can be accessed at https://researchdatafinder.qut.edu.au/display/n7962

References

1. Zádor, J., Taatjes, C.A., Fernandes, R.X.: Kinetics of elementary reactions in low-temperature autoignition chemistry. Prog. Energy Comb. Sci. **37**, 371-421 (2011)

2. Orlando, J.J., Tyndall, G.S.: Laboratory studies of organic peroxy radical chemistry: an overview with emphasis on recent issues of atmospheric significance. Chem. Soc. Rev. **41**, 6294-6317 (2012)

3. Li, R., Smith, R.L., Kenttamaa, H.I.: Fluorine Substitution Enhances the Reactivity of Substituted Phenyl Radicals toward Organic Hydrogen Atom Donors. J. Am. Chem. Soc. **118**, 5056-5061 (1996)

4. Smith, R.L., Kenttamaa, H.I.: A General Method for the Synthesis of Charged Phenyl Radicals in the Gas Phase. J. Am. Chem. Soc. **117**, 1393-1393 (1995)

5. Thoen, K.K., Smith, R.L., Nousiainen, J.J., Nelson, E.D., Kenttamaa, H.I.: Charged Phenyl Radicals. J. Am. Chem. Soc. **118**, 8669 (1996)

6. Petzold, C.J., Nelson, E.D., Lardin, H.A., Kenttamaa, H.I.: Charge-Site Effects on the Radical Reactivity of Distonic Ions. J. Phys. Chem. A. **106**, 9767-9775 (2002)

7. Yu, S.J., Holliman, C.L., Rempel, D.L., Gross, M.L.: The .beta.-distonic ion from the reaction of pyridine radical cation and ethene: a demonstration of high-pressure trapping in Fourier transform mass spectrometry. J. Am. Chem. Soc. **115**, 9676-9682 (1993)

8. Sorrilha, A.E.P.M., Gozzo, F.C., Pimpim, R.S., Eberlin, M.N.: Multiple stage pentaquadrupole mass spectrometry for generation and characterization of gas-phase ionic species. The case of the PyC2H5+· isomers. J. Am. Soc. Mass Spectrom. **7**, 1126-1137 (1996)

9. Harman, D.G., Blanksby, S.J.: Trapping of a tert-adamantyl peroxyl radical in the gas phase. Chem. Commun., 859-861 (2006)

10. Moore, B.N., Blanksby, S.J., Julian, R.R.: Ion–molecule reactions reveal facile radical migration in peptides. Chemical Communications. 5015-5017 (2009)

11. Kirk, B.B., Harman, D.G., Blanksby, S.J.: Direct observation of the gas phase reaction of the cyclohexyl radical with dioxygen using a distonic radical ion approach. J. Phys. Chem. A. **114**, 1446-1456 (2010)

12. Ly, T., Kirk, B.B., Hettiarachchi, P.I., Poad, B.L.J., Trevitt, A.J., da Silva, G., Blanksby, S.J. Phys. Chem. Chem. Phys. **13**, 16314-16323 (2011)

13. Morishetti, K.K., Sripadi, P., Mariappandar, V., Ren, J.: Generation and characterization of distonic dehydrophenoxide radical anions under electrospray and atmospheric pressure chemical ionizations. Int. J. Mass Spectrom. **299**, 169-177 (2011)

14. da Silva, G., Kirk, B.B., Lloyd, C., Trevitt, A.J., Blanksby, S.J.: Concerted HO2 Elimination from alpha-Aminoalkylperoxyl Free Radicals: Experimental and Theoretical Evidence from the Gas-Phase NH2(*)CHCO2(-) + O2 Reaction. J. Phys. Chem. Lett. **3**, 805-811 (2012)

15. Kirk, B.B., Harman, D.G., Kenttamaa, H.I., Trevitt, A.J., Blanksby, S.J.: Isolation and characterization of charge-tagged phenylperoxyl radicals in the gas phase: direct evidence for products and pathways in low temperature benzene oxidation. Phys. Chem. Chem. Phys. **14**, 16719-16730 (2012)

16. Prendergast, M.B., Cooper, P.A., Kirk, B.B., da Silva, G., Blanksby, S.J., Trevitt, A.J.: Hydroxyl radical formation in the gas phase oxidation of distonic 2-methylphenyl radical cations. Phys. Chem. Chem. Phys. **15**, 20577-20584 (2013)

17. Yates, B.F., Bouma, W.J., Radom, L.: Detection of the prototype phosphonium (CH2PH3), sulfonium (CH2SH2) and chloronium (CH2ClH) ylides by neutralization-reionization mass spectrometry: a theoretical prediction. J. Am. Chem. Soc. **106**, 5805-5808 (1984)

18. Yates, B.F., Bouma, W.J., Radom, L.: Distonic radical cations : Guidelines for the assessment of their stability. Tetrahedron. **42**, 6225-6234 (1986)

19. Stirk, K.M., Kiminkinen, L.M., Kenttamaa, H.I.: Ion-molecule reactions of distonic radical cations. Chem. Rev. **92**, 1649-1665 (1992)

20. Williams, P.E., Jankiewicz, B.J., Kenttamaa, H.I.: Properties and reactivity of gaseous distonic radical ions with aryl radical sites. Chem. Rev. **113**, 6949-6985 (2013)

21. Gryn'ova, G., Marshall, D.L., Blanksby, S.J., Coote, M.L.: Switching radical stability by pH-induced orbital conversion. Nature Chem. **5**, 474-481 (2013)

22. Gryn'ova, G., Coote, M.L.: Origin and scope of long-range stabilizing interactions and associated SOMO-HOMO conversion in distonic radical anions. J. Am. Chem. Soc. **135**, 15392-15403 (2013)

23. Maccarone, A.T., Kirk, B.B., Hansen, C.S., Griffiths, T.M., Olsen, S., Trevitt, A.J., Blanksby, S.J.: Direct observation of photodissociation products from phenylperoxyl radicals isolated in the gas phase. J. Am. Chem. Soc. **135**, 9010-9014 (2013)

24. Kobayashi, H., Sonoda, T., Takuma, K.: Reactivity of halogen substituents of p-halogenoperfluoroanilines in acid media. J. Fluorine Chem. **27**, 1-22 (1985)

25. Harman, D.G., Blanksby, S.J.: Investigation of the gas phase reactivity of the 1-adamantyl radical using a distonic radical anion approach. Org. Biomol. Chem. **5**, 3495-3503 (2007)

26. Habicht, S.C., Vinueza, N.R., Archibold, E.F., Penggao, D., Kenttamaa, H.I.: Identification of the carboxylic acid functionality by using electrospray ionization and ion-molecule reactions in a modified linear quadrupole ion trap mass spectrometer. Anal. Chem. **80**, 3416-3421 (2008)

27. Hansen, C.S., Kirk, B.B., Blanksby, S.J., O'Hair, R.A., Trevitt, A.J.: UV photodissociation action spectroscopy of haloanilinium ions in a linear quadrupole ion trap mass spectrometer. J. Am. Soc. Mass Spectrom. **24**, 932-940 (2013)

28. Ly, T., Julian, R.R.: Residue-specific radical-directed dissociation of whole proteins in the gas phase. J. Am. Chem. Soc. **130**, 351-358 (2008)

29. Kim, T.Y., Thompson, M.S., Reilly, J.P.: Peptide photodissociation at 157 nm in a linear ion trap mass spectrometer. Rapid Commun. Mass Spectrom. **19**, 1657-1665 (2005)

30. Gronert, S., Pratt, L.M., Mogali, S.: Substituent Effects in Gas-Phase Substitutions and Eliminations: β-Halo Substituents. Solvation Reverses SN2 Substituent Effects. J. Am. Chem. Soc. **123**, 3081-3091 (2001)

31. Langevin, P.: A fundamental formula of kinetic theory. Ann. Chem. Phys. **5**, 245 (1905)

32. Donald, W.A., Khairallah, G.N., O'Hair, R.A.J.: The effective temperature of ions stored in a linear quadrupole ion trap mass spectrometer. J. Am. Soc. Mass Spectrom. **24**, 811-815 (2013)

33. Gronert, S.: Estimation of effective ion temperatures in a quadrupole ion trap. J. Am. Soc. Mass. Spectrom. **9**, 845-848 (1998)

34. Tolmachev, A.V., Vilkov, A.N., Bogdanov, B., Pasa-Tolic, L., Masselon, C.D., Smith, R.D.: Collisional activation of ions in RF ion traps and ion guides: the effective ion temperature treatment. J. Am. Soc. Mass. Spectrom. **15**, 1616-1629 (2004)

35. Frisch, M.J., Trucks, G.W., Schlegel, H.B., Scuseria, G.E., Robb, M.A., Cheeseman, J.R., Scalmani, G., Barone, V., Mennucci, B., Petersson, G.A., Nakatsuji, H., Caricato, M., Li, X., Hratchian, H.P., Izmaylov, A.F., Bloino, J., Zheng, G., Sonnenberg, J.L., Hada, M., Ehara, M., Toyota, K., Fukuda, R., Hasegawa, J., Ishida, M., Nakajima, T., Honda, Y., Kitao, O., Nakai, H., Vreven, T., Montgomery Jr., J.A., Peralta, J.E., Ogliaro, F., Bearpark, M.J., Heyd, J., Brothers, E.N., Kudin, K.N., Staroverov, V.N., Kobayashi, R., Normand, J., Raghavachari, K., Rendell, A.P., Burant, J.C., Iyengar, S.S., Tomasi, J., Cossi, M., Rega, N., Millam, N.J., Klene, M., Knox, J.E., Cross, J.B., Bakken, V., Adamo, C., Jaramillo, J., Gomperts, R., Stratmann, R.E., Yazyev, O., Austin, A.J., Cammi, R., Pomelli, C., Ochterski, J.W., Martin, R.L., Morokuma, K., Zakrzewski, V.G., Voth, G.A., Salvador, P., Dannenberg, J.J., Dapprich, S., Daniels,

A.D., Farkas, Ö., Foresman, J.B., Ortiz, J.V., Cioslowski, J., Fox, D.J.: Gaussian 09, Revision B.01 Gaussian, Inc., Wallingford, CT, USA (2009)

36. Zhao, Y., Truhlar, D.G.: A new local density functional for main-group thermochemistry, transition metal bonding, thermochemical kinetics, and noncovalent interactions. J. Chem. Phys. **125**, 194101-194118 (2006)

37. Zhao, Y., Truhlar, D.G.: The M06 suite of density functionals for main group thermochemistry, thermochemical kinetics, noncovalent interactions, excited states, and transition elements: two new functionals and systematic testing of four M06-class functionals and 12 other functionals. Theor. Chem. Acc. **120**, 215-241 (2008)

38. Ly, T., Zhang, X., Sun, Q., Moore, B., Tao, Y., Julian, R.R.: Rapid, quantitative, and site specific synthesis of biomolecular radicals from a simple photocaged precursor. Chem. Commun. **47**, 2835-2837 (2011)

39. Stirk, K.M., Orlowski, J.C., Leeck, D.T., Kenttämaa, H.I.: The identification of distonic radical cations on the basis of a reaction with dimethyl disulfide. J. Am. Chem. Soc. **114**, 8604-8606 (1992)

40. Grabowski, J.J., Zhang, L.: Dimethyl disulfide: anion-molecule reactions in the gas phase at 300 K. J. Am. Chem. Soc. **111**, 1193-1203 (1989)

41. Kauw, J., Born, M., Ingemann, S., Nibbering, N.M.M.: Gas-phase Reactions of Isomeric Carbene and Distonic Radical Anions Derived from Methylthioacetonitrile with Dimethyl Disulfide. Rapid Commun. Mass Spectrom. **10**, 1400-1404 (1996)

42. Koenig, T., Smith, M., Snell, W.: The helium(I) photoelectron spectrum of cyclopentadienone. J. Am. Chem. Soc. **99**, 6663-6667 (1977)

43. Prendergast, M.B., Kirk, B.B., Savee, J.D., Osborn, D.L., Taatjes, C.A., Masters, K.-S., Blanksby, S.J., Da Silva, G., Trevitt, A.J.: Formation and stability of gas-phase o-benzoquinone from oxidation of ortho-hydroxyphenyl: a combined neutral and distonic radical study. Phys. Chem. Chem. Phys. **18**, 4320-4332 (2016)

44. Ormond, T.K., Scheer, A.M., Nimlos, M.R., Robichaud, D.J., Troy, T.P., Ahmed, M., Daily, J.W., Nguyen, T.L., Stanton, J.F., Ellison, G.B.: Pyrolysis of Cyclopentadienone: Mechanistic Insights from a Direct Measurement of Product Branching Ratios. J. Phys. Chem. A. **119**, 7222-7234 (2015)

45. Carpenter, B.K.: Computational prediction of new mechanisms for the reactions of vinyl and phenyl radicals with molecular oxygen. J. Am. Chem. Soc. **115**, 9806-9807 (1993)

46. Fadden, M.J., Barckholtz, C., Hadad, C.M.: Computational Study of the Unimolecular Decomposition Pathways of Phenylperoxy Radical. J. Phys. Chem. A. **104**, 3004-3011 (2000)

47. Fadden, M.J., Hadad, C.M.: Unimolecular Decomposition of the 2-Oxepinoxy Radical: A Key Seven-Membered Ring Intermediate in the Thermal Oxidation of Benzene. J. Phys. Chem. A. **104**, 8121-8130 (2000)

48. Carpenter, B.K.: Ring Opening of Dioxiranylmethyl Radical: A Caution on the Use of G2-Type ab Initio MO Methods for Mechanistic Analysis. J. Phys. Chem. A. **105**, 4585-4588 (2001)

49. Kroner, S.M., DeMatteo, M.P., Hadad, C.M., Carpenter, B.K.: The gas-phase acidity of 2(3H)-oxepinone: a step toward an experimental heat of formation for the 2-oxepinoxy radical. J. Am. Chem. Soc. **127**, 7466-7473 (2005)

50. Tokmakov, I.V., Kim, G., Kislov, B.B., Mebel, A.M., Lin, M.C.: The reaction of phenyl radical with molecular oxygen: a G2M study of the potential energy surface. J. Phys. Chem. A. **109**, 6114-6127 (2005)

51. Sebbar, N., Bockhorn, H., Bozzelli, J.W.: Thermodynamic properties of the species resulting from the phenyl radical with O2 reaction system. Int. J. Chem. Kinet. **40**, 583-604 (2008)

52. Grob, C.A., Kaiser, A., Schweizer, T.: The transmission of polar effects. Part II. Helv. Chim. Acta. **60**, 391-399 (1977)

53. Yu, T., Lin, M.C.: Kinetics of the C6H5 + O2 Reaction at Low Temperatures. J. Am. Chem. Soc. **116**, 9571-9576 (1994)

54. Tonokura, K., Norikane, T., Koshi, M., Nakano, Y., Nakamichi, S., Goto, M., Hashimoto, S., Kawasaki, M., Anderson, M.P.S., Hurley, M.D., Wallington, T.J.: Cavity Ring-down Study of the Visible Absorption Spectrum of the Phenyl Radical and Kinetics of Its Reactions with Cl, Br, Cl2, and O2. J. Phys. Chem. A. **106**, 5908-5917 (2002)

55. Tanaka, K., Ando, M., Sakamoto, Y., Tonokura, K.: Pressure dependence of phenylperoxy radical formation in the reaction of phenyl radical with molecular oxygen. Int. J. Chem. Kinet. **44**, 41-50 (2011)

56. Ly, T., Kirk, B.B., Hettiarachchi, P.I., Poad, B.L., Trevitt, A.J., da Silva, G., Blanksby, S.J.: Reactions of simple and peptidic alpha-carboxylate radical anions with dioxygen in the gas phase. Phys. Chem. Chem. Phys. **13**, 16314-16323 (2011)

57. Bright, C.C., Prendergast, M.B., Kelly, P.D., Bezzina, J.P., Blanksby, S.J., da Silva, G., Trevitt, A.J.: Highly efficient gas-phase reactivity of protonated pyridine radicals with propene. Phys. Chem. Chem. Phys. **19**, 31072-31084 (2017)